Atmos. Chem. Phys. Discuss., 10, 24171–24204, 2010
www.atmos-chem-phys-discuss.net/10/24171/2010/
doi:10.5194/acpd-10-24171-2010

Atmospheric Chemistry and Physics Discussions

Sensitivity of stratospheric Br_y to uncertainties in very short lived substance emissions and atmospheric transport

R. Schofield[1], **S. Fueglistaler**[2,*], **I. Wohltmann**[1], **and M. Rex**[1]

[1]Alfred Wegener Institute, Potsdam, Germany
[2]Department of Applied Mathematics and Theoretical Physics, University of Cambridge, Cambridge, UK
[*]now at: Department of Geosciences, Princeton University, New Jersey, USA

Received: 11 September 2010 – Accepted: 5 October 2010 – Published: 18 October 2010

Correspondence to: R. Schofield (robyn.schofield@awi.de)

Published by Copernicus Publications on behalf of the European Geosciences Union.

Abstract

We evaluate the sensitivity of Br_y entering the stratosphere with a simplified model that allows calculations over a wide parameter range for parameters that are currently poorly quantified. The model examines the transport process uncertainties in the source concentrations and lifetimes, in the convective parameterization and in the inorganic bromine washout process due to dehydration. Source concentrations at the surface and lifetimes were found to have a slight effect on the resultant Br_y (~2 ppt), however this was highly dependent upon, with increasing significance, the degree of efficiency of convective delivery. Efficiency of convective delivery of boundary layer (BL) air to the tropical tropopause layer (TTL) along with washout at the CPT were found to significantly affect Br_y at 400 K – altering the delivered Br_y by 3.3 ppt and 2.9 ppt, respectively. We find that the results critically depend on free tropospheric Br_y concentrations due to dilution of convective updrafts, and the processes that control free tropospheric Br_y require further attention.

1 Introduction

Stratospheric measurements of BrO from ground-based, balloon and satellite platforms can only be explained with an additional 3–8 ppt of total reactive bromine (Br_y) to that provided by the long lived bromine containing halons and CH_3Br (Law and Sturges, 2007). The bromine containing very short-lived substances (VSLS), with lifetimes less than 6 months, have been suggested to bridge this shortfall in the stratospheric bromine budget (Sinnhuber et al., 2002, 2005; Schofield et al., 2004, 2006; Salawitch et al., 2005; Dorf et al., 2006; Livesey et al., 2006; Hendrick et al., 2007; Theys et al., 2009).

The transport of VSLS from their sources to the stratosphere is complex, and a model from emission at the surface to stratospheric Br_y that captures all intricacies is not yet realisable. In particular, the following processes have been identified as main sources of uncertainty:

ACPD
10, 24171–24204, 2010

– VSLS source concentrations:
the VSLS have predominantly natural sources, i.e. marine macro-algae. Questions remain about the conditions under which increased bromine VSLS are produced, and therefore which seasons and locations are "hot spots" for bromine VSLS production.

– VSLS lifetimes:
the lifetimes of the VSLS bromocarbons are determined by OH concentrations and photolysis. OH concentrations in the TTL are uncertain but likely lower than in the free troposphere, and consequently VSLS lifetimes may be longer.

– Transport from boundary layer (BL) to the tropical tropopause layer (TTL):
transport within the BL, and the entrainment of BL air into deep convective cells is not well constrained. The modelling of deep convective events is challenging: therefore capturing the timing, location and the proportion of BL air detraining into the TTL remains uncertain.

– Transport and washout in the TTL:
the transport time-scale in the TTL is similar to that of the lifetime of VSLS, such that washout of inorganic product species during dehydration in the TTL may remove a substantial fraction of Br_y prior to entering the stratosphere.

Our study seeks to quantify the relative importance of the (large) uncertainties in each of these steps. We use a lagrangian model with trajectories based on data from the European Centre for Medium-range Weather Forecasts (ECMWF) ERA-Interim data (Simmons et al., 2007) as representation of the global circulation in combination with a simplified representation of the processes affecting VSLS concentrations during transport from troposphere to stratosphere. For each process, the model has a "tuning knob" that allows evaluation of sensitivities. In Sect. 2 the conceptual model setup describing the simplified microphysical and VSLS box model is outlined. In Sect. 3 we discuss the sensitivities of the resultant stratospheric Br_y budget to the

ACPD
10, 24171–24204, 2010

conceptualized chemical, microphysical and convective processes that control the stratospheric bromine budget.

2 Conceptual model set-up

We use the following conceptual model to estimate the total bromine concentration of air entering the stratospheric overworld (i.e. above 380 K potential temperature (Hoskins, 1991)). Trajectories based on data from ERA-Interim are used as the representation of the large-scale circulation. A simple process "box model" is run along the trajectory to represent the effect of deep convection detraining in the TTL, and to calculate the effect of chemical and washout processes on Br_y delivery to the stratosphere. Trajectories are started on 28/2 (DJF), 31/5 (MAM), 31/8 (JJA) and 30/11 (SON) for 2000 through 2005 at 400 K on a 2° latitude × 2° longitude grid between 50° N and 50° S. They are traced backwards in time using the analysed horizontal wind fields and the clear-sky radiative heating rates obtained from the ERA-Interim forecast runs. Trajectories are calculated with a 10 min integration timestep and are saved with a 30 min timestep. Further details of the trajectory model are given by Wohltmann and Rex (2008).

Figure 1 provides a simple pictorial view of the processes controlling the delivery of bromine to the stratosphere. The thick blue line illustrates a 3 month back-trajectory started at 400 K that crosses Θ=365 K. Only trajectories that have crossed 365 K during the 3 months are considered in this study. At t_0, the earliest time of the back trajectory, Br_y^{OrgSL} (the mixing ratio total of bromine atoms in the organic short lived bromine substances or source gases (SG) – χ^{SG}) is initialized with the WMO 2006 recommendations for the upper troposphere (UT) (Law and Sturges, 2007, table 2-2). As the trajectory ascends the TTL, the SG concentrations making up the Br_y^{OrgSL} are increased by convection (see Sect. 2.2 below) which transports a mixture of boundary-layer and free-tropospheric air with corresponding VSLS concentrations. The proportion of the

ACPD
10, 24171–24204, 2010

detrained air of BL origin is given by the efficiency parameter ζ (see Sect. 2.3). ζ is allowed to vary between 0 (no BL organic bromine containing species in convective outflow) to 1 (BL organic bromine containing species detrain undiluted). The Br_y^{OrgSL} SGs are converted to highly soluble product gases (PGs); Br_y^{Inorg}, at a rate that is determined by α. α is derived from the individual SG lifetimes and is suitably adjusted when convective injection of "younger air" occurs (see Sect. 2.4). Br_y^{Inorg} is a catch all for the product species of bromocarbon breakdown, thought to be dominated by HOBr and HBr (85%) in the TTL region, the rest made up from Br_2 and BrO (Yang et al., 2005). The highly soluble Br_y^{Inorg} is accumulated along the trajectory and partly removed from the system at the time of the last dehydration at the trajectory's cold point. The parameter γ determines the efficiency of this washout, with values between 0 (complete retention of the PG) to 1 (complete PG removal of Br_y^{Inorg} at the cold point) as detailed in Sect. 2.5.

2.1 Br_y source budget

The VSLSs bromine species with lifetimes from 3.5 weeks to 5 months, and methyl bromide with a longer lifetime of 0.7 yr are all the species that are thought to contribute to the tropospheric (Yang et al., 2005), hence TTL reactive bromine budget. All of these bromocarbons, along with the long lived halons and how many bromine atoms they contribute are listed in Table 1 and make up the known and potential stratospheric Br_y budget. The VSLS bromocarbons have known oceanic sources from ice algae, macro-algae and phytoplankton, whereas CH_3Br has both natural (oceanic) and anthropogenic (fumigation and biomass burning) sources (Yang et al., 2005).

Figure 2 displays the SG contribution of each of the species to the stratospheric Br_y budget (Br_y^{OrgSL}+Br_y^{Halons}) as a function of time from the initial time of t_0. The rate of decay shown for each species is driven solely by that species' lifetime. The UT background concentration is given in the top panel, from WMO recommendations (Law

ACPD
10, 24171–24204, 2010

and Sturges, 2007). The oceanic and coastal concentrations of the Br_y^{OrgSL} are given for the Yokouchi et al. (2005) emissions (refer to Table 2). The coastal regions which display the highest Br_y^{OrgSL} are defined as 2° latitude × 2° longitude boxes containing both land and ocean.

The two slightly different BL concentration scenarios considered in this work are listed in Table 2. For the first emission scenario oceanic and coastal boundary layer concentrations of CH_2Br_2, $CHBr_3$ and $CHBr_2Cl$ are prescribed from the (purposely selected) high measurements of (Yokouchi et al., 2005). The land values are those given by WMO (2006). The effect of an alternative BL source scenario based upon (Kerkweg et al., 2008) makes up scenario 2. This second scenario has 4 times less $CHBr_3$ in the coastal BL and slightly less CH_2Br_2. In this second scenario the level of the most abundant tropospheric bromine containing species, CH_3Br is increased to 10 ppt, typical of 30° N with no coastal/oceanic or land differences. Higher elevated levels up to 60 ppt have been observed and associated with biomass burning (Andreae et al., 1996).

2.2 Convective mixing

By construction, the pathways of the trajectories do not include vertical transport from convection, as no latent heat release is included in the diabatic rates that are used to derive the vertical transport. Rather, the impact of convection is modeled by explicit mixing with convective air, for which we use the archived 3 hourly ERA-Interim detrainment rates (this calculation is performed offline from the trajectory code, and hence the timestep is given by the trajectory output, i.e. 30 min). Whenever a convective detrainment rate larger than zero is encountered, a fraction of the trajectory's "airmass" is replaced by air with characteristics of the convective detrainment. The path of the trajectory prior to this mixing event can then be thought as being the path of the airmass into which the detrainment has occurred. We express this formally as follows. The fractional change in airmass characteristics, expressed in terms of VSLS source

ACPD
10, 24171–24204, 2010

gas (SG) mixing ratio χ^{SG}, is given by

$$\chi_i^{SG} = (d_c \times \Delta t)\chi_C^{SG} + (1 - d_c \times \Delta t)\chi_{i-1}^{SG} \quad (1)$$

where i denotes the iteration step, Δt is the model timestep, d_c is the normalized convective detrainment rate (i.e. divergence, see Fig. 3), χ_{i-1}^{SG} is the mixing ratio of the SG (organic Br_y) on the trajectory prior to the mixing event, and χ_C is the mixing ratio of the convective outflow. Correspondingly, convective dilution of the product gas (PG: here Br_y^{Inorg}) is calculated by replacing SG with PG in the equation above, however, as no PG is assumed in the convective outflow, χ_C^{PG} is set to zero.

Figure 3 displays the spatial and temporal variability of the detrainment rates for 2000 used in this calculation. Tost et al. (2010) examining uncertainties arising from model convection schemes, including that of ECMWF, found while convective activity within the models studied was often poorly correlated with actual observed events, over longer timescales good agreement was achieved, that is longer-lived CO and O_3 UT concentrations were well modeled but shorter-lived species were not. Conversely, Folkins et al. (2006) argue for a pronounced annual cycle in deep convective detrainment based on ozone measurements, which is clearly not observed here. Therefore, the ERA-Interim detrainment rates provide a convenient, high temporal and spatial resolution measure of convective detrainment, but it has to be borne in mind, that they have an inherent uncertainty that is difficult to quantify.

Figure 4 shows the evolution of airmass along an exemplary trajectory. Note how each mixing event reduces the importance of the characteristics prior to the mixing event – i.e. the system "loses memory". The loss of memory intrinsic to the system studied here reduces the sensitivity of results to the arguably somewhat ad-hoc initialisation in the upper troposphere. Indeed, results become more sensitive to the characteristics of the in-mixed air, a point we further discuss in Sect. 2.3 below. Generally, we find that in our model calculations convective in-mixing occurs prior to the trajectory's cold point, with only one or two weak events after the cold point. (The example shown

ACPD
10, 24171–24204, 2010

in Fig. 4 shows a case of several convective mixing events prior to, and one event after, the cold point.)

The approach chosen here to include the effect of convective in-mixing along a trajectory may be compared to the method of James et al. (2008). The key difference is that here, an individual trajectory eventually represents a spectrum of different convective origin, whereas their approach assigns each trajectory to one single convective event. We find that typically the spectrum of origin is dominated by the contributions from one or two convective events, which can be interpreted as the "most likely point of origin" equivalent to the single event scenario of James et al. (2008). The main difference for the calculation of Br_y of the two approaches arises from the non-linearity of the washout (see below) of inorganic product species, but the impact is less important than, for example, for the modelling of water isotopologues (Dessler et al., 2007) where the two methods yield quite different results (data not shown).

2.3 Convective dilution of BL air (ζ)

The VSLS concentration of the convective outflow is a function of time and position of the convective mixing event. We assume that the convective detrainment represents a mixture of air directly from the boundary layer and entrained free tropospheric air, following the study of Romps and Kuang (2010) who found convective outflow only to comprise of between 10 and 30% of BL air. For the BL, we set the mixing ratio to the BL mixing ratio given by a model based on emission scenarios for land, coastal and oceanic sources either from Yokouchi et al. (2005) or Kerkweg et al. (2008) (see Table 1). For the free troposphere (FT), (χ_{FT}) we use again the values recommended by Law and Sturges (2007). The dilution of fresh boundary layer air χ_{BL} by free tropospheric air χ_{FT} in the convective outflow χ_C is determined by a parameter ζ (ranging from 0 to 1), such that

$$\chi_C = \zeta \chi_{BL}(\phi, \lambda) + (1 - \zeta)\chi_{FT} \quad (2)$$

ACPD
10, 24171–24204, 2010

Through variations in ζ we can determine the sensitivity to efficiency of convection to bring BL air directly into the TTL.

The χ_{BL} is assigned to be land, oceanic or coastal in nature, depending upon the location (latitude $-\phi$ and longitude λ) of the trajectory for that timestep (see Fig. 4). Rather than tracking each species contribution, we keep track of the average age of air and the fraction that comes from land, ocean, coastal or free tropospheric source regions. As pointed out before, for the situation where convective in-mixing is strong, the composition of the airmass eventually entering the stratosphere depends strongly on the characteristics of the "convective" air mass. Since we use the same "free tropospheric" concentrations for convection over land, coast and ocean, the "free tropospheric" concentrations approaches $1-\zeta$ in this limit. This is evident in Fig. 4, where we have used ζ=0.3. Upon reaching a contribution of $1-\zeta$ for free tropospheric air, subsequent convection can only change the partitioning between land, coast and ocean for the fraction ζ.

2.4 Br_y chemical lifetime (α)

In this conceptual model the individual bromine source species are not accounted for separately, only the total organic short lived SGs:Br_y^{OrgSL} and their total degradation PGs (Br_y^{Inorg}) are saved along the trajectories, therefore an "overall" lifetime of Br_y^{OrgSL} that varies with convection is necessary. The individual species' lifetimes used in this work are given in Table 1 (Law and Sturges, 2007), i.e. for bromoform the lifetime is 26 days, which is in the middle of the range 15 to 37 days given by Warwick et al. (2006). α is the total weighted effective lifetime controlling the PG formation rate and is defined here as a concentration weighted lifetime for all the bromine species that have lifetimes shorter than one year (VSLS+CH_3Br). Note that CH_3Br is usually treated as a long lived species within chemistry-climate and transport models and this could lead to erroneous results, as there is some loss of CH_3Br to inorganic bromine (~0.5 ppt, see Fig. 2) after even 15 days (time required for ~80% of ascending trajectories to

ACPD
10, 24171–24204, 2010

reach cold point from 365 K). This could lead to the underestimation of the Br_y deficit that needs to be explained by the VSLS.

The effective age of air upon the trajectory (t') is altered over an iteration as:

$$t'_i = t'_{i-1}\left(1 - \frac{(d_c\Delta t)\chi_C^{SG}}{\chi_i^{SG}}\right) + t'_C\left(\frac{(d_c\Delta t)\chi_C^{SG}}{\chi_i^{SG}}\right) + \Delta t \quad (3)$$

where t'_C is the age of the convectively introduced air (i.e. is zero), therefore the second term is zero. The fractional term in the above equation represents the proportion of VSLS in the trajectory air parcel that was newly introduced by convection. When no convection occurs (i.e. χ_C^{SG}=0) then t'_i=t'_{i-1}+Δt and the air parcel simply ages as expected by the model timestep.

The fraction of air (f) from each source region (land, ocean, coastal and free troposphere) is altered with each convective event and the cumulative lifetime is generated using the age of air and these fractions:

$$\alpha_i = \sum_{j=1}^{n} f_j \times \alpha_j(t') \quad (4)$$

where n is the number of source regions (here 4) and $\alpha(t')$ is the cumulative lifetime for the age of air of the air parcel.

The lifetimes used in this work are for mid-troposphere, so the TTL lifetimes are very likely to be different from these. We expect that lower OH concentrations in the TTL will outweigh the increased photolysis and thereby increase the lifetimes (especially that of CH_2Br_2 which undergoes little photolytic loss (Hossaini et al., 2010)). We explore the effect of increasing the lifetime of CH_3Br as this is the most abundant SG in the 2nd emission scenario run.

ACPD
10, 24171–24204, 2010

α can be viewed as the e-folding lifetime (Gettelman et al., 2009) determining the PG formation rate via SG loss. The formation of PG is given over a timestep by:

$$\chi_i^{\mathrm{PG}} = \chi_{i-1}^{\mathrm{PG}} + \frac{\chi_{i-1}^{\mathrm{SG}}}{\alpha_i}\Delta t \quad (5)$$

where $\Delta t = t_i - t_{i-1}$ is the model timestep. The second term of the right hand side of Eq. (5) represents the loss of the SG to PG; thereby the complementary equation for the degradation of the SG is given as:

$$\chi_i^{\mathrm{SG}} = \chi_{i-1}^{\mathrm{SG}} - \frac{\chi_{i-1}^{\mathrm{SG}}}{\alpha_i}\Delta t \quad (6)$$

α changes (following Eq. 4) as the contributions from different sources via convection, alters the individual species' concentrations, as demonstrated in Fig. 5 by the exemplary trajectories. Convective injection tends to decrease the cumulative lifetime, after 40 days the initial UT Br_y cumulative lifetime would remain at 0.4 yr (~150 days), this is shown to be reduced down to 0.2 yr (~73 days) through convection with the BL convective efficiency parameter set to 30% (see Sect. 2.3).

2.5 Washout of inorganic product species (γ)

Br_y^{Inorg} PG washout within the TTL is accounted for by introducing a parameter γ. As air ascends through the tropical tropopause almost all of the water condenses and is removed. Wet deposition of Br_y^{Inorg} is the largest removal mechanism for bromine containing substances. The question of how the soluble Br_y^{Inorg} interacts with the ice particles is a topic of current research, very relevant for both convective delivery/washout and advective ascent washout. The heterogeneous recycling of Br_y^{Inorg} into insoluble reactive forms has been demonstrated to increase the aerosol/cloud washout times from 6–9 days to 9–15 days at altitudes above 500 hPa (von Glasow et al., 2004). To investigate the relative importance of microphysics within the TTL the term γ varies

ACPD
10, 24171–24204, 2010

between 0 and 1 to represent the fraction of soluble PG (Br_y^{Inorg}) that is simply removed at the CPT:

$$\chi_{CPT}^{Tot} = \chi_{CPT}^{SG} + (1-\gamma) \times \chi_{CPT}^{PG} \quad (7)$$

where χ_{CPT}^{Tot} is the total bromine (Br_y) that survives washout at the CPT, thereby is guaranteed to enter the stratosphere, with only convective input above the CPT increasing this amount. Therefore, γ captures both the uptake efficiency of the aerosol/cloud particles and the heterogeneous recycling to insoluble bromine substances through the TTL. When γ=0 then there is no removal with ice sedimentation at the CPT and the total Br_y (Inorg+Org) that reaches 400 K is just the initialization value altered by convectively introduced Br_y.

3 Discussion

In the following section the effective age of air reaching the CPT, the residence times (Fig. 6) and general properties of TTL transport provided by the back trajectories initiated at 400 K for the four seasons in 2000 are discussed. This is followed by a discussion of the Br_y transport sensitivity tests that look at the role of the sources, convection and washout upon the Br_y arriving at 400 K.

Figure 7 displays the spatial distribution of Br_y arriving at 400 K for year 2000 using ERA-Interim detrainment rates as the convection proxy, BL concentrations defined by Yokouchi et al. (2005), a BL to outflow efficiency of 30% and complete CPT washout. Figure 8 provides the distribution of Br_y over all trajectories that ascend through the TTL 365–400 K, and arrive between 50° N and 50° S, at different stages of transport through the TTL. All of the seasons DJF, MAM, JJA and SON and increasing the convective efficiencies of BL to outflow of ζ=10%, 30% and 50% are displayed.

Figure 9 displays boxplots of the distributions highlighting the sensitivity of the results to season, washout, BL to outflow efficiency, convection after the CPT and source

ACPD
10, 24171–24204, 2010

concentrations/lifetimes. Figure 10 displays the seasonal and interannual variation in the Br_y distribution being delivered to 400 K from 2000–2005. For these multiyear runs the UT initialization of Halons and CH_3Br decrease as prescribed in (WMO, 2006), otherwise the emissions of Yokouchi et al. (2005), ERA-Interim detrainment rates, ζ of 30%, and complete washout of Br_y^{Inorg} at the CPT, are used.

3.1 Residence times

The role of chemical conversion into soluble Br_y^{Inorg} and hence the role of washout on the water soluble Br_y^{Inorg} entering the stratosphere is critically dependent upon the time spent ascending through the TTL and the time since the last convective event. Following Eq. 3, the left panels of Fig. 6 display the effective convection corrected age of air reaching the CPT for each season. The effect of recent convective activity in reducing the effective age is clear. In the boreal winter greater air ages are associated with CPTs north of 10° N and conversely in boreal summer with CPTs south of 10° S. These patterns are anticipated following the seasonal shift of the convective inter-tropical convergence zone (ITCZ) (Fueglistaler et al., 2009).

The right-hand panels of Fig. 6 display the total transit time (residence time) from 365 to 400 K for each season in 2000. Also shown is the trajectory location at 355 K (open circles – nominal TTL "entry point") for all trajectories that reach 400 K with residence times less than 30 days. The TTL entry points for the fastest TTL transport cluster over the Western Pacific/Indonesia region, but a significant proportion also originate from the Indian Ocean and East Africa. This general picture holds for all years from 2000 to 2005.

The total transport times from 365 K to 400 K (Fig. 6 show a seasonal dependence with mean values of 45 days in DJF increasing to ~60 days in JJA, this is in qualitative agreement with the age of air at 17 km reported by Folkins et al. (2006) of 40 days for boreal winter (DJF) and 70 days for boreal summer (JJA). These residence times are significantly longer than trajectory study of Fueglistaler et al. (2004) using the too rapid

ACPD
10, 24171–24204, 2010

vertical winds of ERA-40 which gave a seasonally independent transport time between 340 K and 400 K of about 30 days.

A quarter of all the back-trajectories started at 400 K between 50° N and 50° S fail to run back to 365 K after 3 months. Few of the trajectories reaching 400 K originate at 365 K north of 30° N in DJF and similarly few south of 30° S in JJA – following the inter-tropical convergence zone (ITCZ) latitudinal TTL entry shift with season (Fueglistaler et al., 2009). CPTs are limited between 20° N and 20° S irrespective of season. Figure 7 displays the distinctive hourglass nature of the TTL transport with the neck being defined at the CPT.

3.2 The role of organic bromine emissions

The effect of altering the underlying concentrations of the SLS detrained into the TTL with convection from the two scenarios supplied in Table 2 is displayed in Fig. 9. Emissions from Kerkweg et al. (2008) increase CH_3Br and reduce the concentrations of the shorter-lived $CHBr_3$ and CH_2Br_2 from coastal and oceanic sources relative to those of Yokouchi et al. (2005). The lifetime of CH_3Br is also increased from 0.7 to 1.0 yr consistent with the work of Montzka et al. (2003) and Kerkweg et al. (2008); which suggest a lifetime of $\gg$0.8 and 1 yr, respectively. Such a shift to longer lived species reduces the importance of convection and reduces the magnitude of the seasonality (though it is still evident). The median Br_y arriving at 400 K, is reduced from 21.3 ppt to 20.3 ppt (VSLS 4.8 to 3.8 ppt) and the distribution is considerably narrowed by changing the underlying emission sources and lifetime. However, the drastically different BL emission scenarios have a much smaller impact on stratospheric Br_y than one might have expected. This is because the FT convectively entrains with a factor of 0.7 and more (Romps and Kuang, 2010) and a constant VSLS concentration independent of the location of convection, thereby strongly attenuating the impact of BL source strength and geographical patterns. No claim is made here that the assumption of a single typical free tropospheric VSLS concentration is valid. Rather, the assumption is made only because of lack of measurements of the global distribution of VSLS in the free

ACPD
10, 24171–24204, 2010

troposphere. Our result highlights the need for more measurements and to focus future model studies on the FT mixing component of the system, to better constrain how FT VSLS is influenced by BL emissions.

Recent modelling combined with measurements studies have investigated the contribution of the bromine VSLS of bromoform ($CHBr_3$) and dibromomethane (CH_2Br_2) (Sinnhuber and Folkins, 2006; Laube et al., 2008; Aschmann et al., 2009; Gettelman et al., 2009; Hossaini et al., 2010; Liang et al., 2010) upon the stratospheric Br_y budget. As Fig. 2 shows these two species are the dominant among the bromine VSLSs, but $CHBr_2Cl$ may also be important. The most abundant substance – CH_3Br, due to its relative rapid decay and source fluctuations, also needs to be taken into account in SLS studies attempting to reconcile the stratospheric Br_y budget.

3.3 The role of convection

Br_y transport across the TTL for all seasons is displayed spatially in Fig. 7 for a convective efficiency ζ=30% and quantitatively in Figs. 8–10.

The difference between the blue and green curves of Fig. 8 illustrates the effect of convection above 365 K on Br_y (no washout) – shifting the distribution peak by 1–2 ppt (note: loss of the initialization peak at 21 ppt). The convective influence after the CPT is given by the difference between red and teal curves in Fig. 8 and is small (0.4 ppt difference in median values). This finding is in line with the findings of Aschmann et al. (2009), who found negligible change when convection above 380 K was switched off.

Figure 9 shows that for a convective efficiency ζ of 30% in DJF, Br_y reaching 400 K has a median value of an additional 4.8 ppt. This is lower than the 6–7 ppt tropical maximum of Br_y modelled by Warwick et al. (2006) with a complexer emission pattern than the simple high source concentrations for ocean and coastal areas used here.

Changing the BL to outflow convection efficiency from 10% to 50% shows a broadening of the Br_y distribution reaching 400 K and increasing the median value from 19.6 ppt to 22.9 ppt (VSLS 3.1 ppt to 6.4 ppt), with a distribution spanning the higher end of the required +8 ppt inferred from BrO measurements (Law and Sturges, 2007) – indicated

ACPD
10, 24171–24204, 2010

by the grey shading in Fig. 9. A 50% BL component of the convective outflow, however, is not supported by the study of Romps and Kuang (2010), rather the difference between 10 and 30%: Br_y increasing from 19.6 ppt to 21.3 ppt (VSLS 3.1 ppt to 4.8 ppt), shows this is a key sensitivity.

3.4 Role of CPT washout

Br_y^{Inorg} available for washout is displayed in the middle panels of Fig. 7. In Fig. 8 the role of washout is seen as the difference between the green and teal curves. From Fig. 9 washout reduces the Br_y that would arrive at 400 K from 24.2 to 21.3 ppt (VSLS 7.7 ppt to 4.8 ppt). Thus washout removes 38% of the Br_y at the CPT, this is (not surprisingly) lower than the 50% found by Aschmann et al. (2009) considering only the most short-lived substance $CHBr_3$.

Complete non-washout results in a stratospheric Br_y concentration distribution marginally consistent only with observations at the higher end of the range of stratospheric BrO (Sinnhuber et al., 2002, 2005; Schofield et al., 2004, 2006; Salawitch et al., 2005; Dorf et al., 2006; Livesey et al., 2006; Hendrick et al., 2007; Theys et al., 2009). We expect that washout is effective – with HOBr and HBr being very soluble species constituting 85% of the Br_y^{Inorg} in the TTL (Yang et al., 2005). We can therefore eliminate the possibility that no washout occurs, but 15% retention would result in 0.5 ppt more Br_y arriving at 400 K, this would be indistinguishable from increased source concentrations or a slight increase in BL to TTL convective efficiency.

As there is little seasonality in the ERA-Interim detrainment rates and no seasonality in the sources in this study, the seasonality seen in Fig. 9 arises from washout timing (residence times) and ITCZ seasonal shift in the TTL transport (as found also in the study of Liang et al., 2010). Washout is most effective in DJF with a mean loss of 2.9 ppt, and least effective in JJA with only 2.4 ppt lost, (MAM and SON having mean losses 2.4 and 2.5, respectively). Under no washout (i.e. purely ITCZ driven), DJF and MAM receive mean Br_y concentrations of 24.2 ppt, this is followed by SON with 24.1 ppt and JJA with 23.8 ppt. Therefore, the resultant seasonality is complicated:

ACPD
10, 24171–24204, 2010

DJF, while receiving more convective injection of Br_y succumbs to higher washout, exactly opposite to JJA where less convective injection of Br_y occurs and less washout. Thereby washout at the CPT acts to dampen any convectively introduced seasonality. The seasonality in Figs. 9 and 10 displays this complicated, almost flat behavior. The tape-recorder seasonality seen by Aschmann et al. (2009) in soluble Br_y above the CPT with a maxima in boreal summer is not therefore supported by this work. Figure 8 shows that a mean value of 3.1 ppt: 15% of the Br_y at 400 K exists in the inorganic form for all seasons except SON where Br_y^{Inorg} at 400 K is only 2.3 ppt (11%) of the total, resulting from the fast upper TTL transport times in this season.

4 Conclusions

With this conceptual study, we have been able to explore the sensitivity of Br_y arriving at 400 K due to emission sources, convection and washout. We conclude:

- When the emissions convected are longer lived, the resultant distributions are narrower, with a lower mean value. Determining the TTL OH field will be vital in constraining the TTL lifetimes of the SLS, and therefore determining the source importance.
- The efficiency with which BL organic Br_y source gases are delivered to the convective outflow is very important – 1.7 ppt additional Br_y results as the efficiency is increased from 10 to 30% (the expected range from Romps and Kuang, 2010).
- With the chemical composition of the convective outflow being dominated by that of in-mixed free tropospheric air, the stratospheric Br_y budget is critically affected by the processes that control the free tropospheric VSLS, in particular to what extent the geographic distributions of free tropospheric VSLS are controlled by large-scale transport versus local emissions.

ACPD
10, 24171–24204, 2010

- We find that the seasonal migration of the ITCZ and the seasonal cycle in residence time both produce a corresponding seasonality in Br_y delivery to the stratosphere, but that the two cycles are out of phase and hence largely cancel. A larger seasonality of stratospheric Br_y may be expected if deep convective outflow would have a substantial seasonality. This seasonality however would be expected to be dampened if the washout displays a higher efficiency at colder temperatures.
- Convection after the cold point plays a minor role (0.4 ppt), though higher sensitivities are achieved with high convective efficiencies and higher BL VSLS concentrations.
- No washout of Br_y^{Inorg} at the CPT results in a distribution that is at the higher end of inferences of Br_y from stratospheric BrO measurements.

Convective dilution has an extreme influence upon the significance of BL emissions, therefore obtaining of accurate free tropospheric SG concentrations is vital in future studies. Another source of uncertainty is the assumption that FT delivers 0 PG: is this a reasonable assumption given the well-mixed nature and high moisture situation, or could PGs be expected to be delivered with convective ice lofting?

Despite the simplistic nature and coarse assumptions made in this study, the widths of the Br_y distributions arriving 400 K are narrower than the VSLS contribution to the stratospheric Br_y budget range of 3–8 ppt suggested from BrO measurements (Law and Sturges, 2007). Establishing emission sources, their TTL lifetimes, the amount of BL air within the convective outflow and the efficiency of the washout process are the areas which require better constraints in reconciling the Br_y budget with BrO measurements. The convective detrainment rates provide an vital component of this system, we require an improvement in our understanding of the expected depths and seasonality. Improvement in our observational knowledge of the total stratospheric Br_y (i.e. reducing the current VSLS 3–8 ppt uncertainty range) will also significantly aid in the process of understanding stratospheric Br_y, hence our ability to make long term stratospheric ozone projections.

ACPD
10, 24171–24204, 2010

Acknowledgements. We thank I. Folkins for useful discussions. The authors thank ECMWF for providing ERA-Interim data via special project DERESI. Funding support for this work was provided by the European Union (EU) funded WaVES (MIF1-CT-2006-039646), SCOUT-O3 (GOCE-CT-2004-505390) and SHIVA (2008-226224) projects.

References

Andreae, M. O., Atlas, E., Harris, G. W., Helas, G., deKock, A., Koppmann, R., Maenhaut, W., Manø, S., Pollock, W. H., Rudolph, J., Scharffe, D., Schebeske, G., and Welling, M.: Methyl halide emissions from savanna fires in Southern Africa, J. Geophys. Res., 101(D19), 23603–23613, 1996. 24176

Aschmann, J., Sinnhuber, B.-M., Atlas, E. L., and Schauffler, S. M.: Modeling the transport of very short-lived substances into the tropical upper troposphere and lower stratosphere, Atmos. Chem. Phys., 9, 9237–9247, doi:10.5194/acp-9-9237-2009, 2009. 24185, 24186, 24187

Dessler, A. E., Hanisco, T. F., and Fueglistaler, S.: Effects of convective ice lofting on H_2O and HDO in the tropical tropopause layer, J. Geophys. Res., 112, D18309, doi:10.1029/2007JD008609, 2007. 24178

Dorf, M., Butler, J. H., Butz, A., Camy-Peyret, C., Chipperfield, M. P., Kritten, L., Montzka, S. A., Simmes, B., Weidner, F., and Pfeilsticker, K.: Long-term observations of stratospheric bromine reveal slow down in growth, Geophys. Res. Lett., 33, L24803, doi:10.1029/2006gl027714, 2006. 24172, 24186

Folkins, I., Bernath, P., Boone, C., Lesins, G., Livesey, N., Thompson, A. M., Walker, K., and Witte, J. C.: Seasonal cycles of O-3, CO, and convective outflow at the tropical tropopause, Geophys. Res. Lett., 33, L16802, doi:10.1029/2006GL026602, 2006. 24177, 24183

Fueglistaler, S., Wernli, H., and Peter, T.: Tropical troposphere-to-stratosphere transport inferred from trajectory calculations, J. Geophys. Res., 109, D03108, doi:10.1029/2003JD004069, 2004. 24183

Fueglistaler, S., Dessler, A. E., Dunkerton, T. J., Folkins, I., Fu, Q., and Mote, P. W.: Tropical tropopause layer, Rev. Geophys., 47, RG1004, doi:10.1029/2008rg000267, 2009. 24183, 24184

Gettelman, A., Lauritzen, P. H., Park, M., and Kay, J. E.: Processes regulating short-

ACPD

10, 24171–24204, 2010

lived species in the tropical tropopause layer, J. Geophys. Res., 114, D13303, doi:10.1029/2009jd011785, 2009. 24181, 24185

Hendrick, F., Van Roozendael, M., Chipperfield, M. P., Dorf, M., Goutail, F., Yang, X., Fayt, C., Hermans, C., Pfeilsticker, K., Pommereau, J.-P., Pyle, J. A., Theys, N., and De Mazière, M.: Retrieval of stratospheric and tropospheric BrO profiles and columns using ground-based zenith-sky DOAS observations at Harestua, 60° N, Atmos. Chem. Phys., 7, 4869–4885, doi:10.5194/acp-7-4869-2007, 2007. 24172, 24186

Hoskins, B. J.: Towards a PV-Theta view of the general-circulation, Tellus, 43(4), 27–35, 1991. 24174

Hossaini, R., Chipperfield, M. P., Monge-Sanz, B. M., Richards, N. A. D., Atlas, E., and Blake, D. R.: Bromoform and dibromomethane in the tropics: a 3-D model study of chemistry and transport, Atmos. Chem. Phys., 10, 719–735, doi:10.5194/acp-10-719-2010, 2010. 24180, 24185

James, R., Bonazzola, M., Legras, B., Surbled, K., and Fueglistaler, S.: Water vapor transport and dehydration above convective outflow during Asian monsoon, Geophys. Res. Lett., 35, L20810, doi:10.1029/2008GL035441, 2008. 24178

Kerkweg, A., Jöckel, P., Warwick, N., Gebhardt, S., Brenninkmeijer, C. A. M., and Lelieveld, J.: Consistent simulation of bromine chemistry from the marine boundary layer to the stratosphere – Part 2: Bromocarbons, Atmos. Chem. Phys., 8, 5919–5939, doi:10.5194/acp-8-5919-2008, 2008. 24176, 24178, 24184, 24194

Laube, J. C., Engel, A., Bönisch, H., Möbius, T., Worton, D. R., Sturges, W. T., Grunow, K., and Schmidt, U.: Contribution of very short-lived organic substances to stratospheric chlorine and bromine in the tropics – a case study, Atmos. Chem. Phys., 8, 7325–7334, doi:10.5194/acp-8-7325-2008, 2008. 24185

Law, K. S. and Sturges, W. T.: Halogenated very short-lived substances, chap. 2, World Meteorological Organization, Geneva, Switzerland, 572 pp., 2007. 24172, 24174, 24175, 24178, 24179, 24185, 24188, 24196

Liang, Q., Stolarski, R. S., Kawa, S. R., Nielsen, J. E., Douglass, A. R., Rodriguez, J. M., Blake, D. R., Atlas, E. L., and Ott, L. E.: Finding the missing stratospheric Br_y: a global modeling study of $CHBr_3$ and CH_2Br_2, Atmos. Chem. Phys., 10, 2269–2286, doi:10.5194/acp-10-2269-2010, 2010. 24185, 24186

Livesey, N. J., Kovalenko, L. J., Salawitch, R. J., MacKenzie, I. A., Chipperfield, M. P., Read, W. G., Jarnot, R. F., and Waters, J. W.: EOS Microwave Limb Sounder observations

ACPD
10, 24171–24204, 2010

of upper stratospheric BrO: implications for total bromine, Geophys. Res. Lett., 33, L20817, doi:10.1029/2006gl026930, 2006. 24172, 24186

Montzka, S. A., Butler, J. H., Hall, B. D., Mondeel, D. J., and Elkins, J. W.: A decline in tropospheric organic bromine, Geophys. Res. Lett., 30(15), 1826, doi:10.1029/2003gl017745, 2003. 24184

Romps, D. M. and Kuang, Z. M.: Do undiluted convective plumes exist in the upper tropical troposphere?, J. Atmos. Sci., 67(2), 468–484, doi:10.1175/2009jas3184.1, 2010. 24178, 24184, 24186, 24187

Salawitch, R. J., Weisenstein, D. K., Kovalenko, L. J., Sioris, C. E., Wennberg, P. O., Chance, K., Ko, M. K. W., and McLinden, C. A.: Sensitivity of ozone to bromine in the lower stratosphere, Geophys. Res. Lett., 32, L05811, doi:10.1029/2004GL021504, 2005. 24172, 24186

Schofield, R., Kreher, K., Connor, B. J., Johnston, P., Thomas, A., Shooter, D., Chipperfield, M., Rodgers, C. D., and Mount, G.: Retrieved tropospheric and stratospheric BrO columns over Lauder, New Zealand, J. Geophys. Res., 109, D14304, doi:10.1029/2003JD004463, 2004. 24172, 24186

Schofield, R., Johnston, P. V., Thomas, A., Kreher, K., Connor, B. J., Wood, S., Shooter, D., Chipperfield, M. P., Richter, A., von Glasow, R., and Rodgers, C. D.: Tropospheric and stratospheric BrO columns over Arrival Heights, Antarctica, 2002, J. Geophys. Res., 111, D22310, doi:10.1029/2005JD007022, 2006. 24172, 24186

Simmons, A. J., Uppala, S., Dee, D., and Kobayashi, S.: ERA interim: new ECMWF reanalysis products from 1989 onwards, ECMWF Newsl., 110, 25–35, 2007. 24173

Sinnhuber, B.-M. and Folkins, I.: Estimating the contribution of bromoform to stratospheric bromine and its relation to dehydration in the tropical tropopause layer, Atmos. Chem. Phys., 6, 4755–4761, doi:10.5194/acp-6-4755-2006, 2006. 24185

Sinnhuber, B. M., Arlander, D. W., Bovensmann, H., Burrows, J. P., Chipperfield, M. P., Enell, C. F., Frieß, U., Hendrick, F., Johnston, P. V., Jones, R. L., Kreher, K., Mohamed-Tahrin, N., Müller, R., Pfeilsticker, K., Platt, U., Pommereau, J, P., Pundt, I., Richter, A., South, A., Tørnkvist, K. K., Van Roozendael, M., Wagner, T., and Wittrock, F.: Comparison of measurements and model calculations of stratospheric bromine monoxide, J. Geophys. Res., 107(D19), 4398, doi:10.1029/2001JD000940, 2002. 24172, 24186

Sinnhuber, B. M., Rozanov, A., Sheode, N., Afe, O. T., Richter, A., Sinnhuber, M., Wittrock, F., Burrows, J. P., Stiller, G. P., von Clarmann, T., and Linden, A.: Global observations of stratospheric bromine monoxide from SCIAMACHY, Geophys. Res. Lett., 32, L20810,

ACPD

10, 24171–24204, 2010

doi:10.1029/2005GL023839, 2005. 24172, 24186

Theys, N., Van Roozendael, M., Errera, Q., Hendrick, F., Daerden, F., Chabrillat, S., Dorf, M., Pfeilsticker, K., Rozanov, A., Lotz, W., Burrows, J. P., Lambert, J.-C., Goutail, F., Roscoe, H. K., and De Mazière, M.: A global stratospheric bromine monoxide climatology based on the BASCOE chemical transport model, Atmos. Chem. Phys., 9, 831–848, doi:10.5194/acp-9-831-2009, 2009. 24172, 24186

Tost, H., Lawrence, M. G., Brühl, C., Jöckel, P., The GABRIEL Team, and The SCOUT-O3-DARWIN/ACTIVE Team: Uncertainties in atmospheric chemistry modelling due to convection parameterisations and subsequent scavenging, Atmos. Chem. Phys., 10, 1931–1951, doi:10.5194/acp-10-1931-2010, 2010. 24177

von Glasow, R., von Kuhlmann, R., Lawrence, M. G., Platt, U., and Crutzen, P. J.: Impact of reactive bromine chemistry in the troposphere, Atmos. Chem. Phys., 4, 2481–2497, doi:10.5194/acp-4-2481-2004, 2004. 24181

Warwick, N. J., Pyle, J. A., Carver, G. D., Yang, X., Savage, N. H., O'Connor, F. M., and Cox, R. A.: Global modeling of biogenic bromocarbons, J. Geophys. Res., 111, D24305, doi:10.1029/2006jd007264, 2006. 24179, 24185

WMO: Scientific assessment of ozone depletion, 2006: report of the Montreal Protocol Scientific Assessment Panel, Tech. rep., WMO Global Ozone Research and Monitoring Project – Report No. 50, 2006. 24176, 24183, 24193, 24202, 24203, 24204

Wohltmann, I. and Rex, M.: Improvement of vertical and residual velocities in pressure or hybrid sigma-pressure coordinates in analysis data in the stratosphere, Atmos. Chem. Phys., 8, 265–272, doi:10.5194/acp-8-265-2008, 2008. 24174

Yang, X., Cox, R. A., Warwick, N. J., Pyle, J. A., Carver, G. D., O'Connor, F. M., and Savage, N. H.: Tropospheric bromine chemistry and its impacts on ozone: a model study, J. Geophys. Res., 110, D23311, doi:10.1029/2005jd006244, 2005. 24175, 24186

Yokouchi, Y., Hasebe, F., Fujiwara, M., Takashima, H., Shiotani, M., Nishi, N., Kanaya, Y., Hashimoto, S., Fraser, P., Toom-Sauntry, D., Mukai, H., and Nojiri, Y.: Correlations and emission ratios among bromoform, dibromochloromethane, and dibromomethane in the atmosphere, J. Geophys. Res., 110, D23309, doi:10.1029/2005jd006303, 2005. 24176, 24178, 24182, 24183, 24184, 24194, 24203, 24204

ACPD

10, 24171–24204, 2010

Table 1. Br_y contributing organic source gases initialized for the base of the TTL Θ=365 K. Halons and CH_3Br as prescribed from table 8-5 WMO (2006) for year 2000 and VSLS species as given by the upper limit of the observed range table 2-2 WMO (2006).

Species	UT Conc [ppt]	Lifetime [yr (days)]	Number Br atoms
Halon1301	2.71	65	1
Halon1211	4.01	16	1
Halon2402	0.41	20	2
Halon1202	0.05	2.9	2
CH_3Br	8.90	0.7 (256)	1
CH_2Br_2	1.0	0.33 (121)	2
$CHBr_3$	0.7	0.07 (26)	3
$CHBr_2Cl$	0.12	0.19 (69)	2
CH_2BrCl	0.35	0.41 (150)	1
$CHBrCl_2$	0.15	0.21 (77)	1

ACPD
10, 24171–24204, 2010

Table 2. Br_y contributed by the SLS in convective outflow. Scenario 1 is based on Yokouchi et al. (2005) and scenario 2 upon Kerkweg et al. (2008).

	Yokouchi et al. (2005)				Kerkweg et al. (2008)			
	Land [ppt]	Coast [ppt]	Ocean [ppt]	τ [yr]	Land [ppt]	Coast [ppt]	Ocean [ppt]	τ [yr]
CH_3Br	8.90	8.90	8.90	0.7	10.0	10.0	10.0	1.0
CH_2Br_2	0.9	3.2	2.0	0.33	1.0	2.2	1.8	0.33
$CHBr_3$	0.37	16.5	3.0	0.07	0.6	4.0	2.0	0.07
$CHBr_2Cl$	0.08	1.6	0.5	0.19	0.08	1.6	0.5	0.19
CH_2BrCl	0.32	0.32	0.32	0.41	0.32	0.32	0.32	0.41
$CHBrCl_2$	0.12	0.12	0.12	0.21	0.12	0.12	0.12	0.21

ACPD
10, 24171–24204, 2010

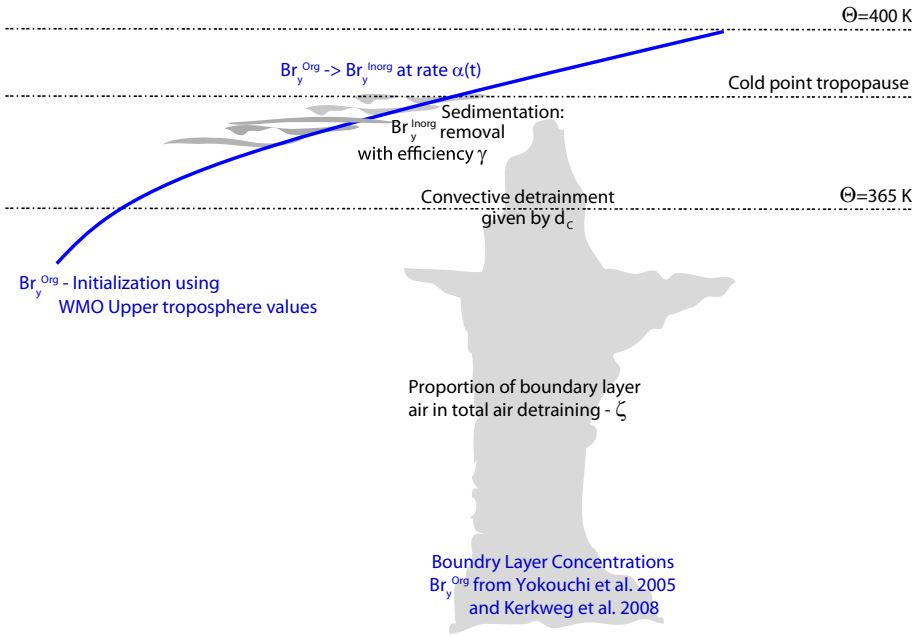

Fig. 1. Schematic illustration of the conceptualised model. The blue line is a single trajectory depicting a "typical" air parcel traversing 365–400 K. Each air parcel trajectory may be subjected to convective injection of organic bromine, delivered from the BL with an efficiency ζ (between 0 and 1). From t_0 inorganic bromine forms via the loss of VSL organic bromine species at an overall rate given by α, determined cumulatively from all of VSL bromine species' lifetimes. As the air parcel dehydrates (forming cirrus) at cold temperatures, the available inorganic bromine washes out with an efficiency γ (between 0 and 1). After the CPT is crossed possible additional convectively injected organic bromine contributes to the total amount of bromine reaching 400 K.

ACPD
10, 24171–24204, 2010

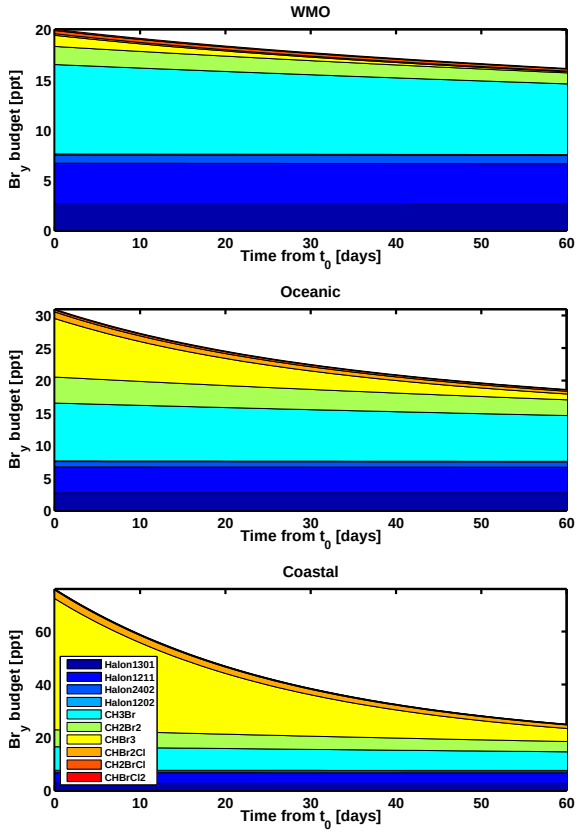

Fig. 2. The source gas contribution of bromine containing substances to the stratospheric Br_y budget from t_0 (entrance time in the TTL). The upper panel provides VSLS concentrations for the upper troposphere as provided in the WMO report (Law and Sturges, 2007). The middle panel and the lower panel give feasible oceanic and coastal concentrations for the VSLS, respectively.

ACPD
10, 24171–24204, 2010

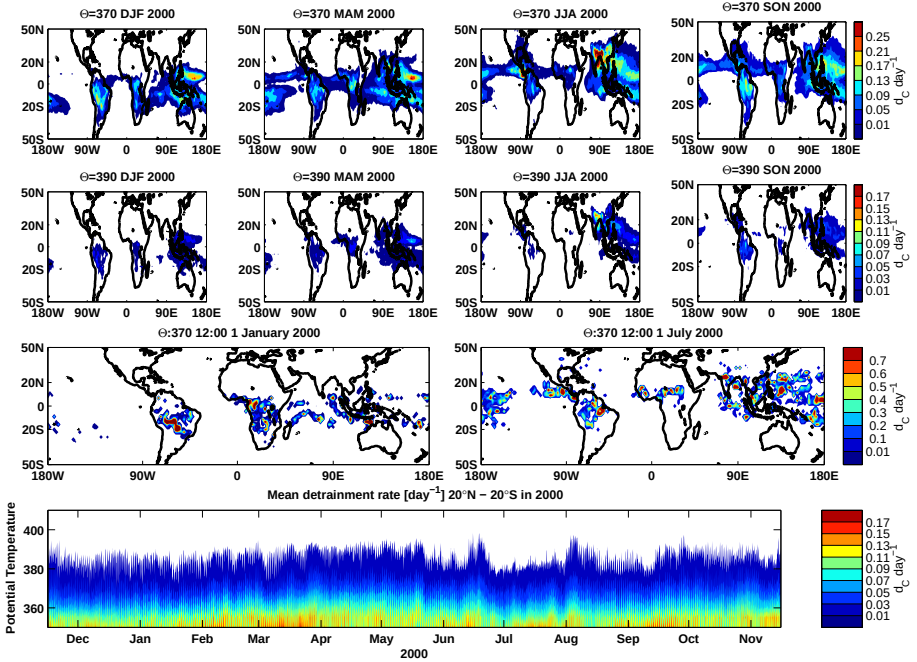

Fig. 3. Spatial and altitude distribution of ERA-Interim detrainment rates. 1st row: Seasonal mean of the detrainment rates at 370 K for December 1999 to February 2000, March to May 2000, June to August 2000 and September to November 2000, 2nd row: same for 390 K. 3rd row gives examples of the detrainment rates at Θ=370 for the 1 January and the 1 July. 4th row shows the temporal variation of the zonal mean between 20° S–20° N for 2000 with altitude.

ACPD
10, 24171–24204, 2010

Sensitivity study of stratospheric Br_y

R. Schofield et al.

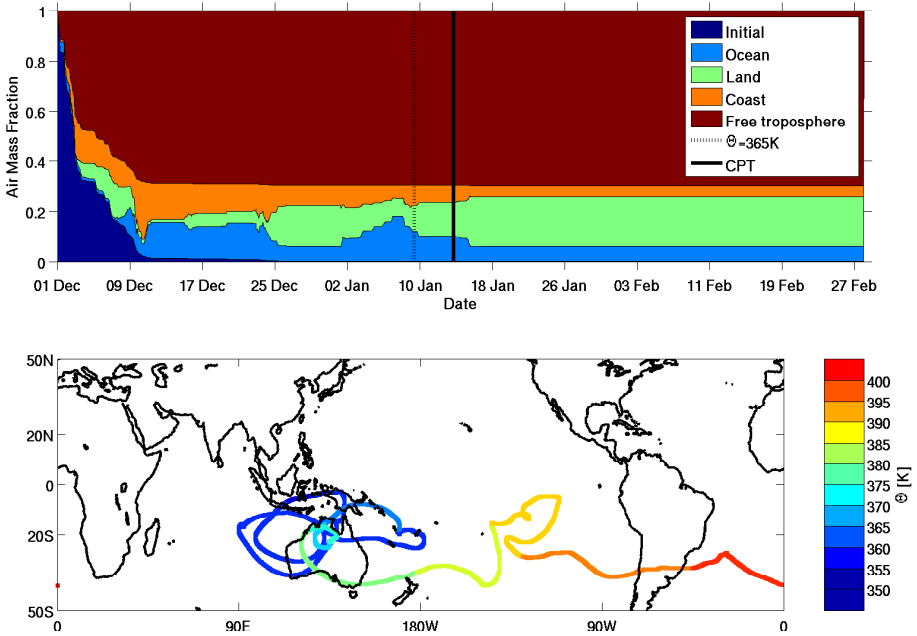

Fig. 4. How convection alters the airmass of an exemplary trajectory for DJF, 2000 is displayed in the upper panel, broken-down into the origin of the replacement air (ζ, the BL component of convective outflow is set at 30%). Where Θ=365 K and the CPT occur are indicated with the dashed and solid lines, respectively. The lower panel displays the trajectory path, with the colour designating the potential temperature of the trajectory.

ACPD
10, 24171–24204, 2010

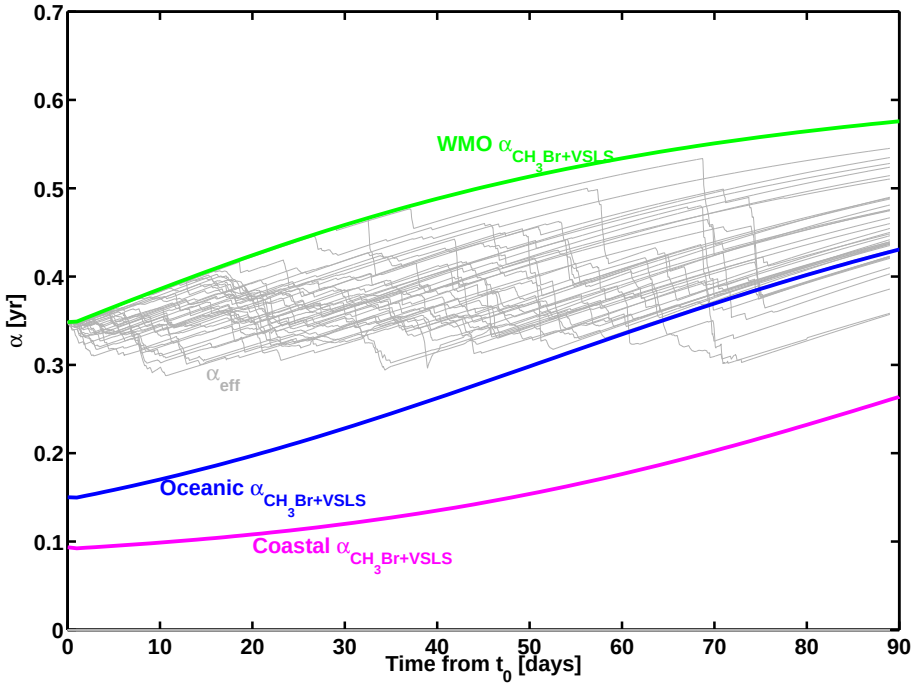

Fig. 5. The cumulative lifetime (α) in years of the short-lived bromine substances for the WMO upper troposphere (green), oceanic (blue) and coastal (magneta) regions from the concentration curves displayed in Fig. 2. In light grey 50 exemplary trajectory changing cumulative lifetimes are displayed – showing how convection from different source regions changes the α values (as the VSLS composition changes).

ACPD
10, 24171–24204, 2010

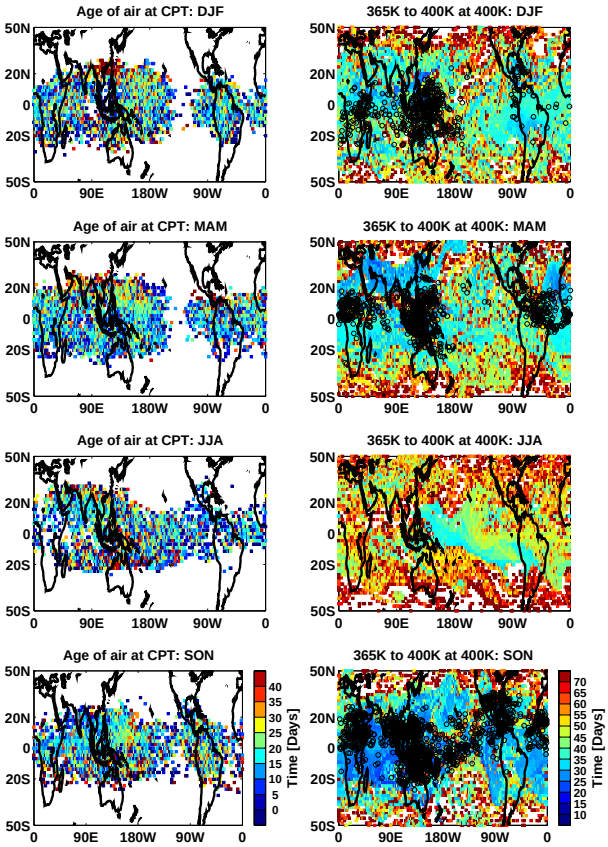

Fig. 6. Map of effective age of the air reaching the CPT at the CPT (left panels) for trajectories traversing the TTL in 2000 for all seasons. The right hand panels display the residence times from 365 K to 400 K at 400 K. The black open circles in the right-hand panels display the trajectory locations at 355 K if the residence times 365–400 K are shorter than 30 days.

ACPD
10, 24171–24204, 2010

Sensitivity study of stratospheric Br_y

R. Schofield et al.

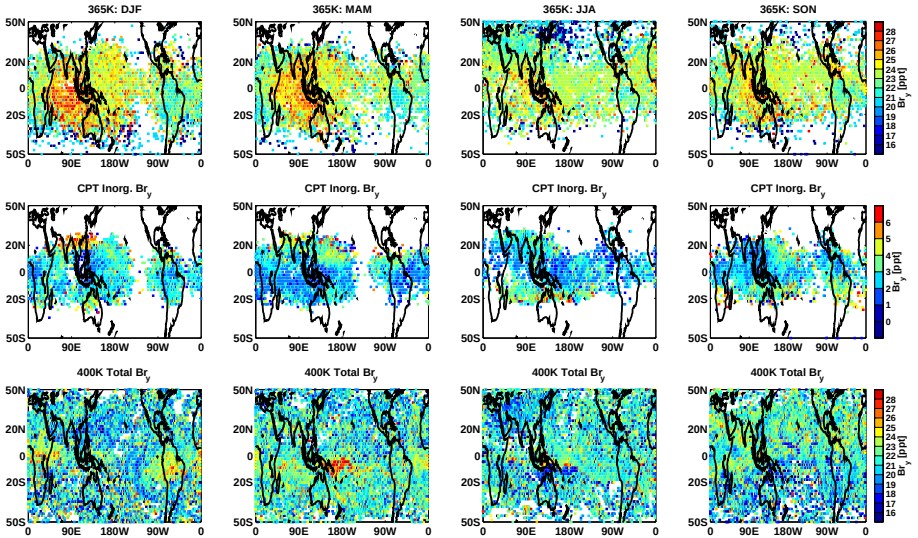

Fig. 7. Br_y transport across the TTL for all seasons. Top row of panels give the spatial distribution of the total Br_y (Br_y^{Inorg}+Br_y^{OrgSL}) at Θ=365 K – i.e. the convective influence before this level. The second row of panels provides the spatial distribution of the amount of Br_y that is in an inorganic form at the cold point. The third row of panels give the spatial distribution of the total Br_y at Θ=400 K.

ACPD
10, 24171–24204, 2010

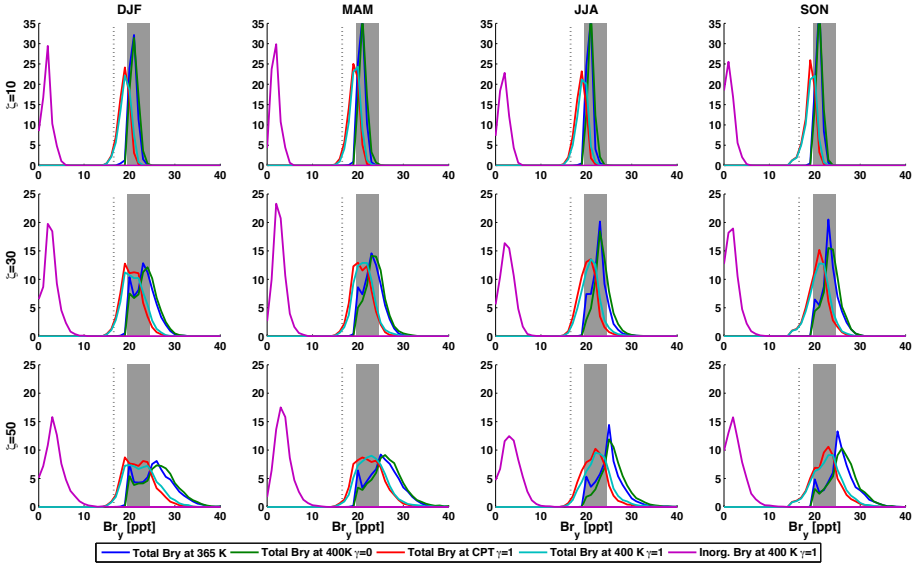

Fig. 8. The distribution over all trajectories of Br_y (% of total trajectories) at Θ=365 K (blue) and at Θ=400 K with γ=1 (teal), and the resultant distributions at 400 K when no washout (γ=0) at the CPT is assumed (green), and at the CPT when γ=1, which is the same as the distribution at Θ=400 K when no convection above the CPT is assumed (red). The total Br_y^{Inorg} at 400 K is also provided (magneta). The dashed line provides the Halons+CH_3Br contribution, and the grey shaded region the WMO recommendation for Halons+CH_3Br+VSLS substances of 3–8 ppt WMO (2006). The top row is for a convective efficiency of 10%, middle row 30% and bottom row 50% over all 4 seasons.

ACPD
10, 24171–24204, 2010

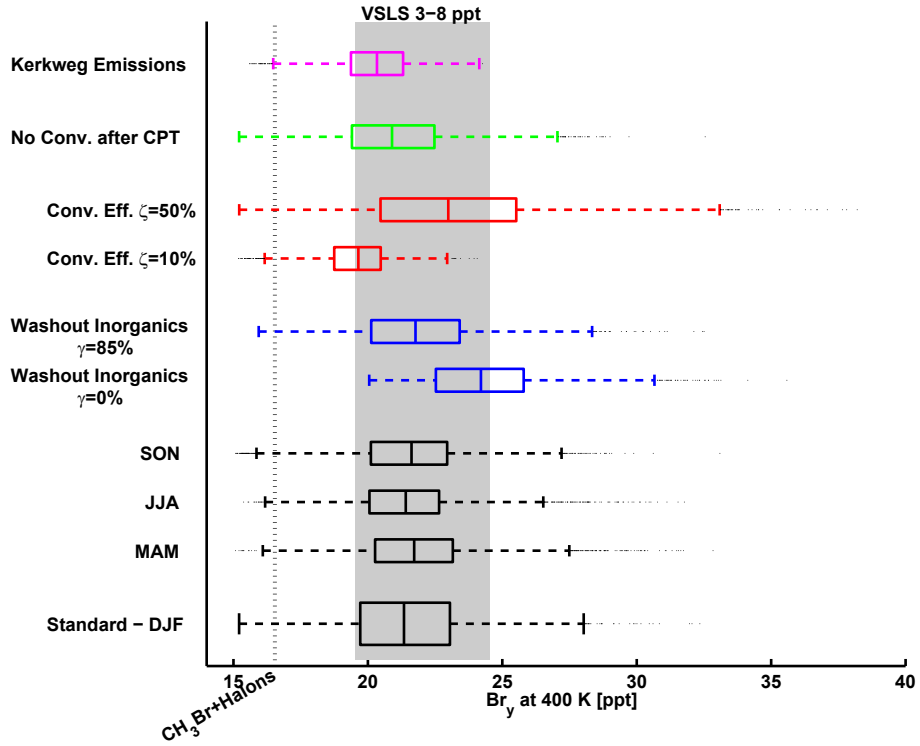

Fig. 9. Boxplots illustrating the different distributions arising for Br_y arriving at 400 K from all trajectories traversing the TTL. The boxes illustrate the 25th to 75th percentiles, the whiskers 1.5× the interquartile range and the crosses outliers. Unless otherwise stated the distributions are for DJF, using Yokouchi et al. (2005) boundary layer concentrations, ζ (boundary layer to outflow) efficiency of 30%, and washout at the CPT of 100%. The lowermost bar is this standard case, and all other bars show the sensitivity to the resultant Br_y for the given indicated change. The dashed line provides the Halons+CH_3Br contribution, and the grey shaded region the WMO recommendation for Halons+CH_3Br+VSLS substances of 3–8 ppt (WMO, 2006).

ACPD
10, 24171–24204, 2010

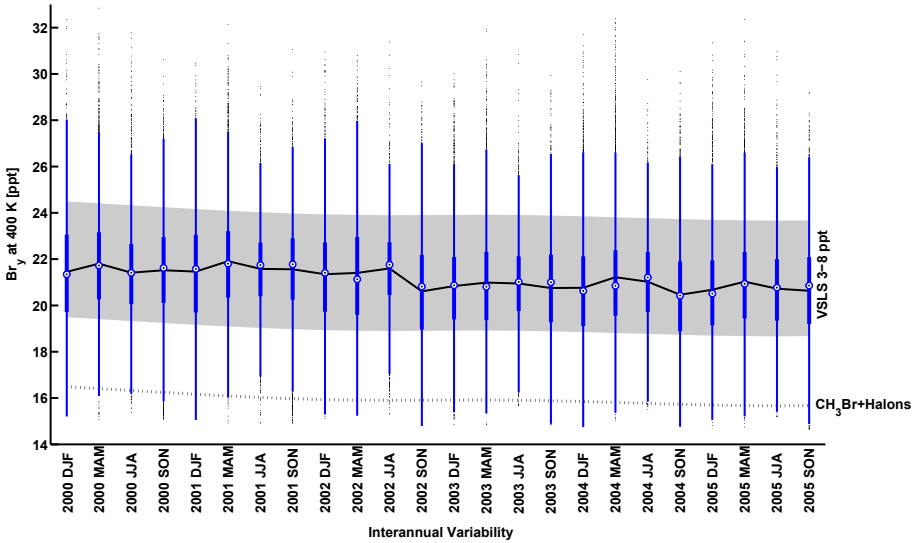

Fig. 10. Boxplots displaying the interannual variability of the distributions of Br_y arriving at 400 K from all trajectories traversing the TTL. The boxes illustrate the 25th to 75th percentiles, the whiskers 1.5× the interquartile range and the crosses outliers. All seasons from 2000 to 2005 are displayed using Yokouchi et al. (2005) boundary layer concentrations, ζ (boundary layer to outflow) efficiency of 30%, and washout at the CPT of 100%. The mean values for each year are given by the solid black line. The dashed line provides the Halons+CH_3Br contribution (with the prescribed decreasing trend), and the grey shaded region the WMO recommendation for Halons+CH_3Br+VSLS substances of 3–8 ppt (WMO, 2006).

ACPD
10, 24171–24204, 2010